

# High-spin structures of $^{136}_{54}\text{Xe}$ , $^{137}_{55}\text{Cs}$ , $^{138}_{56}\text{Ba}$ , $^{139}_{57}\text{La}$ , and $^{140}_{58}\text{Ce}$ : A shell model description

**P.C. Srivastava**

Instituto de Ciencias Nucleares, Universidad Nacional Autónoma de México, 04510 México, D.F., Mexico

E-mail: [praveen.srivastava@nucleares.unam.mx](mailto:praveen.srivastava@nucleares.unam.mx)

**M.J. Ermatov**

Instituto de Ciencias Nucleares, Universidad Nacional Autónoma de México, 04510 México, D.F., Mexico and

Institute of Nuclear Physics, Ulughbek, Tashkent 100214, Uzbekistan

**Irving O. Morales**

Instituto de Ciencias Nucleares, Universidad Nacional Autónoma de México, 04510 México, D.F., Mexico

## Abstract.

In the present work recently available experimental data [A. Astier *et al*, Phys. Rev. C **85**, 064316 (2012)] for high-spin states of five  $N = 82$  isotones,  $^{136}_{54}\text{Xe}$ ,  $^{137}_{55}\text{Cs}$ ,  $^{138}_{56}\text{Ba}$ ,  $^{139}_{57}\text{La}$ , and  $^{140}_{58}\text{Ce}$  have been interpreted with state-of-the-art shell model calculations. The calculations have been performed in the 50-82 valence shell composed of  $1g_{7/2}$ ,  $2d_{5/2}$ ,  $1h_{11/2}$ ,  $3s_{1/2}$ , and  $2d_{3/2}$  orbitals. We have compared our results with the available experimental data for excitation energies including high-spin states, occupancy numbers and transition probabilities. As expected the structure of these isotones are due to proton excitations across  $Z = 50$  shell. The structure of the positive-parity states are mainly from  $(\pi g_{7/2} \pi d_{5/2})^n$  and  $(\pi g_{7/2} \pi d_{5/2})^{n-2} (\pi h_{11/2})^2$  configurations, while the negative-parity states have  $(\pi g_{7/2} \pi d_{5/2})^n (\pi h_{11/2})^1$  configuration. Additionally, for the  $^{136}_{54}\text{Xe}$ ,  $^{137}_{55}\text{Cs}$  and  $^{138}_{56}\text{Ba}$  isotones the excitation of the neutrons across  $N = 82$  gap is important.

PACS numbers: 21.60.Cs, 27.60.+j

## 1. Introduction

Shell structure near doubly magic nuclei is important for the study of weak interaction rates. One of the  $N = 82$  isotones,  $^{136}\text{Xe}$  is a candidate of neutrinoless double beta decay, for determining neutrino mass [1]. For the  $N = 82$  isotones low and high-spin states produced by the spontaneous fission were reported in the literature [2, 3, 4, 5]. Recently, Astier *et al* [6] populated the high-spin states of  $^{136}_{54}\text{Xe}$ ,  $^{137}_{55}\text{Cs}$ ,  $^{138}_{56}\text{Ba}$ ,  $^{139}_{57}\text{La}$ , and  $^{140}_{58}\text{Ce}$  isotopes using fusion-fission reactions.

The aim of this work is to the study  $N = 82$  isotones including several newly populated high-spin states by Astier *et al* [6] within framework of shell model. This would add more comprehensive information to the earlier shell model studies in Refs. [2, 3]. The importance of  $g_{7/2}$ ,  $d_{5/2}$  and  $h_{11/2}$  protons orbitals are crucial in this study. This can be seen from the evaluation of experimental values of the proton occupation number of the ground states for the different orbitals in the even  $N = 82$  isotones in Fig. 1.

Previously, in this region we have analyzed experimentally observed slow  $E3$  transition in  $^{136}\text{Cs}$  at ISOLDE facility at CERN within framework of shell model [7]. Shell model results on the spectroscopic properties of  $fp$  and  $fp_g$  shell nuclei were reported in our earlier works [8, 9, 10]. The  $B(E2)$  transitions trends in the tin isotopes using generalized seniority approach have recently been reported by I. O. Morales *et al* [11].

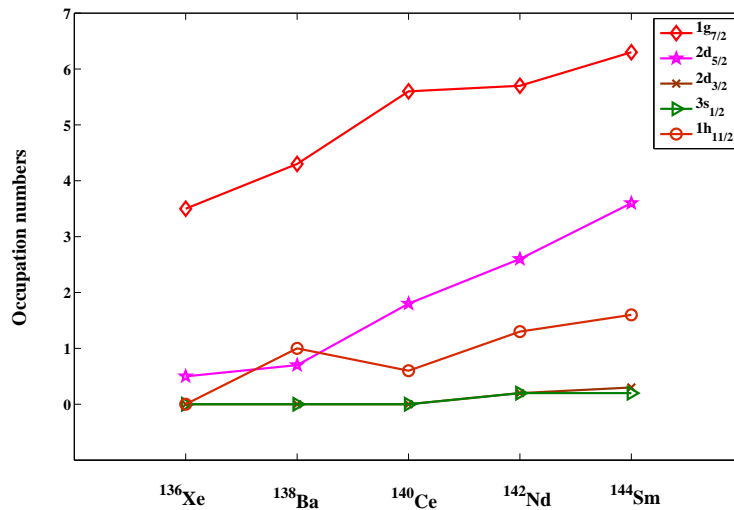


**Figure 1.** Variation of experimental occupation numbers [12] for the ground states for even-mass  $N = 82$  isotones.

This work is organized as follows: comprehensive comparison of shell-model results and experimental data is given in Section 2. In Section 3, transition probabilities are compared with the available experimental data. Finally, concluding remarks are drawn in Section 4.

## 2. Shell model results and discussions

The shell-model calculations for the  $N=82$  isotones have been performed in the 50-82 valence shell composed of the orbits  $1g_{7/2}$ ,  $2d_{5/2}$ ,  $1h_{11/2}$ ,  $3s_{1/2}$ , and  $2d_{3/2}$ . The excited states are mainly due to proton excitations. The full shell-model calculation we have performed with SN100PN interaction due to Brown *et al* [13]. This interaction has four parts: neutron-neutron, neutron-proton, proton-proton and Coulomb repulsion between the protons. The single-particle energies for the neutrons are -10.610, -10.290, -8.717, -8.716, and -8.816 MeV for the  $1g_{7/2}$ ,  $2d_{5/2}$ ,  $2d_{3/2}$ ,  $3s_{1/2}$ , and  $1h_{11/2}$  orbitals, respectively, and those for the protons are 0.807, 1.562, 3.316, 3.224, and 3.603 MeV [7]. The results shown in this work were obtained with the code NuShell [14].

### 2.1. Analysis of spectra

For the  $N = 82$  isotones proton excitations are important among the  $1g_{7/2}$ ,  $2d_{5/2}$ ,  $2d_{3/2}$ ,  $3s_{1/2}$ , and  $1h_{11/2}$  orbitals, above  $Z = 50$  shell closure. The neutrons will not contribute in the structure of these nuclei because of the  $N = 82$  shell closure. In this section we perform shell model calculations for the chain of isotones  $^{136}_{54}\text{Xe}$ ,  $^{137}_{55}\text{Cs}$ ,  $^{138}_{56}\text{Ba}$ ,  $^{139}_{57}\text{La}$ , and  $^{140}_{58}\text{Ce}$ , with valence protons in 50-82 shell in order to describe positive and negative-parity levels of these nuclei. In Table 1 the proton occupancy numbers calculated with shell model are given. They are compared with the available experiment for the even isotones. For the odd isotones, we have listed predictions of the shell model. Results are in very good agreement with the available experimental data. There are 4 to 7 protons in average in  $g_{7/2}$  and  $d_{5/2}$  orbitals. Probability that one proton occupies  $d_{3/2}$  orbital is small and even smaller for  $s_{1/2}$  orbital, which will be seen also from the discussions below.

**2.1.1.  $^{136}_{54}\text{Xe}$ :** Comparison of the calculated values with the experimental data is shown in Fig. 2. Recently, positive-parity levels of  $^{136}\text{Xe}$  are extended up to 7.9 MeV in the experiment [6]. There are also four experimental measured negative-parity levels.

First four calculated positive-parity levels are in a very good agreement with the experiment. The  $6_2^+$  is predicted by SM 239 keV lower than in the experiment. The experimentally observed  $0_2^+$  level is much higher than the calculated  $0_2^+$  level, however it is very close to the calculated  $0_3^+$  level. The levels  $2_2^+$ ,  $2_3^+$ ,  $4_2^+$  and  $4_3^+$  at 2290, 2415, 2465 and 2560 keV are predicted by shell model at 2229, 2358, 2139, and 2261 keV, respectively. The predicted  $8_1^+$  level differs from the experimental one by only 22 keV. The difference increase up to 240 keV for the level  $8_2^+$  at 3228 keV. The  $10_1^+$  level at 3483 keV is predicted by shell model at 3220 keV. The  $8_3^+$  is more than 1 MeV lower in the SM calculation. According to shell model in the states  $0_1^+$ ,  $2_1^+$ ,  $4_1^+$ ,  $6_1^+$  and  $8_1^+$  all four protons prefer to be in  $g_{7/2}$  orbital with 53.3, 63.6, 68.8, 66.4 and 84.1% probabilities, respectively. The newly measured level  $10_2^+$  in [6] is very close to the  $10_3^+$  in the calculation. There are the level sequence  $10_2^+$ ,  $9_1^+$  and  $9_2^+$  levels between the levels  $8_3^+$  and  $10_3^+$  in the calculation which do not exist in the experiment. The rest higher

**Table 1.** Experimental [12] and calculated occupation numbers for the ground states of the  $N = 82$  isotones.

	$\pi g_{7/2}$	$\pi d_{5/2}$	$\pi h_{11/2}$	$\pi d_{3/2}$	$\pi s_{1/2}$	$\pi g_{7/2} + \pi d_{5/2}$
<sup>136</sup> Xe						
Expt.	3.5(4)	0.5(2)	0.0(7)	0.0(2)	0.0(2)	4.0(6)
SM	2.97	0.59	0.29	0.11	0.04	3.56
<sup>137</sup> Cs						
Expt.	-	-	-	-	-	-
SM	3.78	0.75	0.30	0.12	0.04	4.53
<sup>138</sup> Ba						
Expt.	4.3(4)	0.7(3)	1.0(8)	0.0(2)	0.0(2)	5.0(7)
SM	3.98	1.22	0.53	0.19	0.07	5.20
<sup>139</sup> La						
Expt.	-	-	-	-	-	-
SM	4.56	1.58	0.56	0.21	0.09	6.14
<sup>140</sup> Ce						
Expt.	5.6(3)	1.8(2)	0.6(4)	0.0(2)	0.0(2)	7.4(5)
SM	4.75	2.00	0.82	0.29	0.13	6.75

spin states are more compressed in the calculation. The level  $16_1^+$  is predicted much lower than in the experiment. SM predicts larger values for the  $12_1^+$ ,  $13_1^+$ ,  $14_1^+$ ,  $14_2^+$ ,  $15_1^+$ ,  $16_1^+$  and  $17_1^+$  levels. One proton promotion from  $g_{7/2}$  to  $d_{5/2}$  gives  $10_1^+$  with 93.3% probability. The structure of the  $12_1^+$ ,  $14_1^+$  and  $16_1^+$  states are connected with exciting two protons from  $g_{7/2}$  to  $h_{11/2}$  orbital with more than 90% probabilities.

For the negative-parities,  $9^-$  state is the lowest in the experiment while in calculation  $3^-$  is the lowest one. The sequence of the other remained negative-parity levels is the same as in the experiment and these levels are located lower than in the experiment. Three protons are in  $g_{7/2}$  and one proton is in  $h_{11/2}$  for the negative-parity levels up to  $13^-$  with 50.2, 81.4, 94.9 and 96.5% probabilities, respectively. The probability of  $g_{7/2}^2 d_{5/2}^1 h_{11/2}^1$  configuration is 99.7% for the  $14^-$  level. With this model space we predict results up to  $16^+$ .

**2.1.2. <sup>137</sup><sub>55</sub>Cs:** The high-spin level scheme of the odd proton nucleus <sup>137</sup>Cs has been extended up to  $\sim 7.6$  MeV excitation energy and spin (37/2+) [6]. As is seen from Fig. 3 only the sequence of the levels  $1/2_1^+$  and  $1/2_2^+$  is different from the experiment up to  $23/2_1^+$ . Both of them are predicted lower than in the experiment. There are two levels, to which spins are not assigned in the experiment, between the levels ( $23/2_1^+$ ) and ( $19/2_3^+$ ). The next two levels ( $19/2_3^+$ ) and ( $21/2_2^+$ ) are predicted  $\sim 1$  MeV lower by the calculation. Spin is not assigned to the newly measured level at 4699 keV between the levels ( $21/2_2^+$ ) and ( $23/2_2^+$ ). This may be  $21/2_3^+$  according to the shell

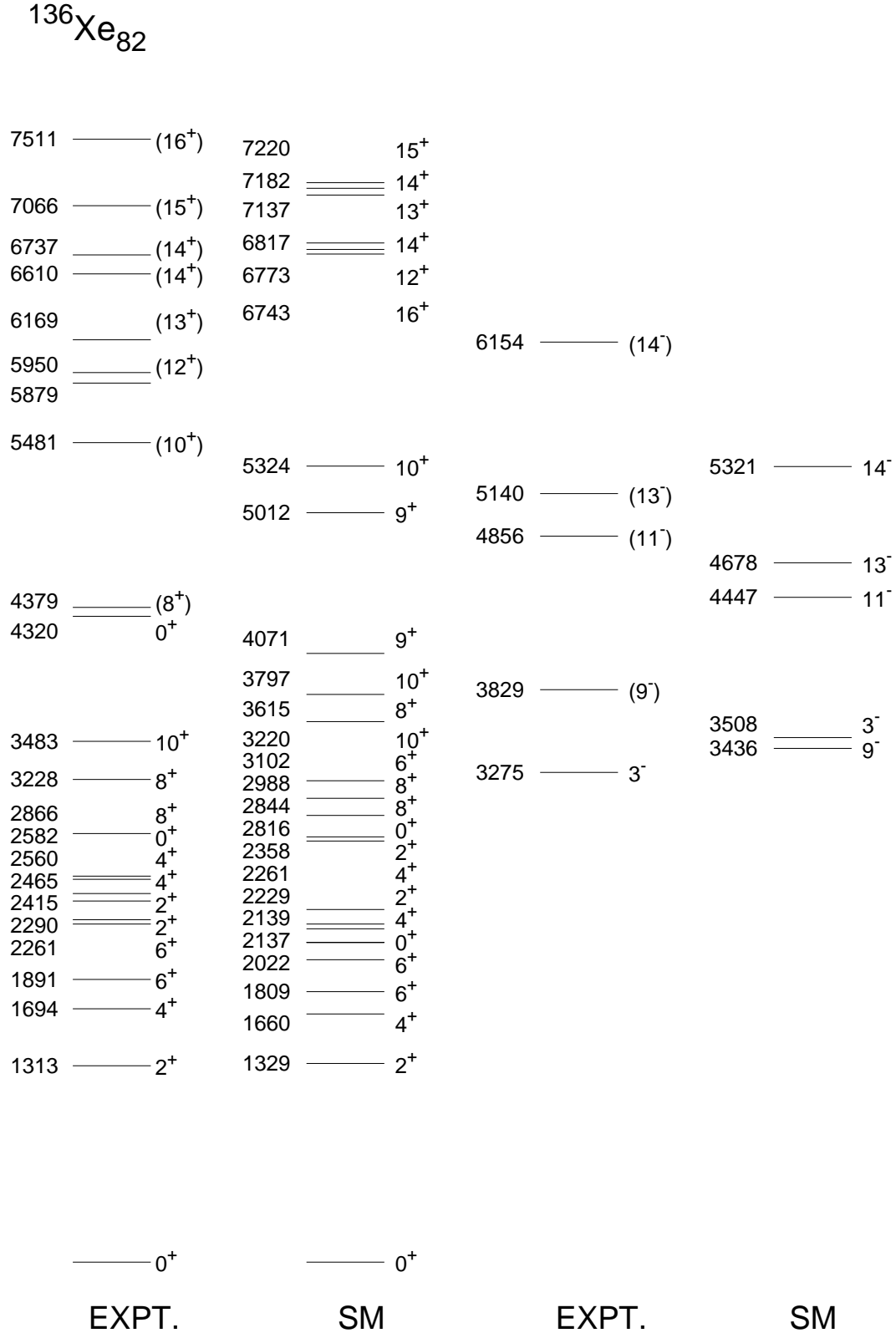


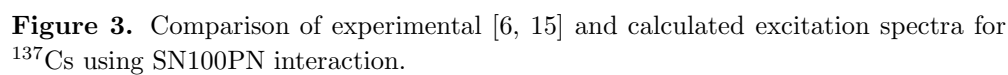
**Figure 2.** Comparison of experimental [6, 15] and calculated excitation spectra for  $^{136}\text{Xe}$  using SN100PN interaction.

model calculation. The highest state ( $37/2_1^+$ ) is predicted by calculation 725 keV lower than in the experiment. The  $7/2_1^+$ ,  $9/2_1^+$ ,  $11/2_1^+$  and  $15/2_1^+$  states are produced by 5 protons in  $g_{7/2}$  orbital with 45.4, 48.3, 51.8 and 47.4% probabilities, respectively. The  $1/2_1^+$ ,  $5/2_1^+$ ,  $13/2_1^+$ ,  $17/2_1^+$ ,  $19/2_1^+$  and  $21/2_1^+$  states are due to one proton promotion from  $g_{7/2}$  to  $d_{5/2}$  in the previous configuration with 40.7, 63.4, 80.4, 79.5, 86.9 and 92.7% probabilities, respectively. For the  $1/2_1^+$  state also contribution of  $g_{7/2}^4 s_{1/2}^1$  configuration is essential: it is predicted by 23.6% probability. The level  $23/2_1^+$  is produced by two proton excitations from  $g_{7/2}$  to  $d_{5/2}$ . Three and two protons are respectively in  $g_{7/2}$  and  $h_{11/2}$  orbitals in producing  $17/2_1^+$ ,  $25/2_1^+$ ,  $27/2_1^+$ ,  $29/2_1^+$ ,  $31/2_1^+$ ,  $33/2_1^+$  and  $35/2_1^+$  levels.

The calculated  $9/2^-$  level is  $\sim 1$  MeV higher than the experimental one. The next triple of the negative-parity states are located very close to each other both in the experiment and calculation. The  $21/1^-$  and  $23/2^-$  states are interchanged with respect to the experiment. The  $27/2^-$  comes after around  $\sim 1$  MeV gap both in the experiment and calculation. The next calculated level is  $25/2^-$  which is not measured in the experiment. The calculated  $29/2^-$  and  $31/2^-$  levels are located lower as compared to the experiment. The spacing between these two levels is less than the experimental one. We have also shown other calculated levels in order to compare with the experimental tentative levels at 5459, 5766, 6554 and 6866 keV. For the negative-parity levels  $9/2^-$ ,  $19/2^-$ ,  $21/2^-$ ,  $23/2^-$ ,  $25/2^-$  and  $27/2^-$  there are 3 protons in  $g_{7/2}$  and 1 in the  $h_{11/2}$  with 61.2, 83.3, 78.9, 77.8, 91.9 and 93.9% probabilities. One proton excitation from  $g_{7/2}$  to  $d_{5/2}$  in the previous structure gives the  $29/2^-$  and  $31/2^-$  levels with 98.0 and 97.8% probabilities, respectively. The levels  $33/2^-$ ,  $35/2^-$  and  $37/2^-$  have configuration  $g_{7/2}^2 h_{11/2}^3$  with 99.3, 98.8 and 97.6% probabilities, respectively.

**2.1.3.  $^{138}_{56}\text{Ba}$ :** Experimental positive-parity levels are available up to  $\sim 9$  MeV excitation energy and spin  $20^+$  for this nucleus [6]. Comparison of the calculated levels with the experimental data is presented in Fig. 4. We have compared three eigenvalues with the experiment up to  $10^+$ . The  $2_1^+$  and  $4_1^+$  are predicted by the calculation only with 4 and 27 keV difference, respectively. In the calculation there is  $0_2^+$  at 1942 keV between  $4_1^+$  and  $6_1^+$  which is at 2340 keV in the experiment. The difference between the experiment and calculation increases up to  $\sim 1.3$  MeV when reaching  $20_1^+$  state. The  $0_1^+$ ,  $2_1^+$ ,  $4_1^+$ ,  $10_1^+$  and  $12_1^+$  levels have  $g_{7/2}^4 d_{5/2}^2$  configuration with 34.6, 40.0, 34.2, 48.5, and 91.7% probabilities. There are five protons in  $g_{7/2}$  and one in  $d_{5/2}$  orbital for the  $6_1^+$  and  $8_1^+$  levels with 42.6 and 54.8% probabilities, respectively. One proton promotion from the previous configuration to  $d_{3/2}$  orbital gives  $13_1^+$  state with 97.3% probability. The  $14_1^+$ ,  $15_1^+$ ,  $16_1^+$  and  $17_1^+$  levels are due to the  $g_{7/2}^4 h_{11/2}^2$  configuration with 87.2, 86.1, 81.5 and 94.1% probabilities, respectively.

The calculated negative-parity levels we have shown up to  $19_1^-$  in order to compare results also with experimentally tentative levels at 7402 and 8011 keV beyond  $17^-$ . It can be noted that as we move from  $^{136}\text{Xe}$  to  $^{138}\text{Ba}$  the calculation now predicts correct order of the  $3^-$  and  $9^-$  as in the experiment. This is due to the change of configuration from  $g_{7/2}^3 h_{11/2}^1$  to  $g_{7/2}^4 d_{5/2}^1 h_{11/2}^1$ . The spacing between these levels are still less than in the



experiment. Negative-parity states are produced because of the odd number of protons in  $h_{11/2}$  orbital. The  $9^-$ ,  $11^-$  and  $13^-$  levels are due to  $g_{7/2}^5 h_{11/2}^1$  configuration with 50.6, 62.8, 65.8 and 81.3% probabilities. The promotion of one proton from  $g_{7/2}$  to  $d_{5/2}$  in the previous configuration gives the  $3^-$ ,  $14^-$  and  $16^-$  levels with 60.2, 81.3 and 94.6% probabilities. For  $17_1^-$  now there is one more proton excitation from  $g_{7/2}$  to  $d_{5/2}$ . In  $19/2^-$  state three protons are both in  $g_{7/2}$  and  $h_{11/2}$  orbital with 96.7% probability.

**2.1.4.  $^{139}_{57}\text{La}$ :** The calculated positive- and negative-parity levels of  $^{139}\text{La}$  are given in Fig. 5. All calculated levels are lower as compared to the experimental ones. The first calculated  $5/2^+$  is closely located to the ground state as compared to the experimental one. The experimental levels from  $1/2^+$  to  $17/2^+$  are located between 1209 and 2032 keV energy range, while calculated energies are between 1004 and 1800 keV. The levels from  $17/2^+$  to  $21/2^+$  come after  $\sim 900$  keV gap in both experiment and calculation. The next sequence of the levels  $23/2^+$  to  $27/2^+$  are located after  $\sim 800$  keV gap both in the experiment and calculation. The sequence of these levels are the same both in the experiment and calculation. For this nucleus  $7/2_1^+$ ,  $11/2_1^+$ ,  $15/2_1^+$ ,  $19/2_1^+$ ,  $23/2_1^+$  and  $27/2_1^+$  states are due to five protons in  $g_{7/2}$  and remained two protons in  $d_{5/2}$  for the first five states and in  $h_{11/2}$  for the last state with 38.6, 51.6, 46.9, 79.5, 82.5 and 60.6% probabilities, respectively. The  $5/2_1^+$ ,  $9/2_1^+$ ,  $13/2_1^+$  and  $17/2_1^+$  states have  $g_{7/2}^6 h_{11/2}^1$  configuration with 32.9, 34.2, 41.7 and 37.8% probabilities. There are four and three protons in  $g_{7/2}$  and  $d_{3/2}$  orbitals for the  $21/2_1^+$  and  $25/2_1^+$  states with 70.7 and 92.9% probabilities, respectively.  $1/2_1^+$  state is due to  $g_{7/2}^4 d_{5/2}^2 s_{1/2}^1$  configuration with 23.8% probability.

The calculated negative-parity levels are in reasonable agreement with the experiment. For the all negative-parity levels one proton is in  $h_{11/2}$ . For the  $11/2^-$  and  $19/2^-$  levels, the remained six protons are in  $g_{7/2}$  with 30.9 and 41.1% probabilities, respectively. Further, the  $g_{7/2}^4 d_{5/2}^1 h_{11/2}^1$  configuration gives the structure for the  $21/2^-$ ,  $25/2^-$  and  $27/2^-$  levels with 39.0, 77.8 and 49.3% probabilities, respectively. The  $23/2^-$  is connected with the configuration where one more proton is moved from  $g_{7/2}$  to  $d_{5/2}$  in the previous configuration with 38.9% probability.

**2.1.5.  $^{140}_{58}\text{Ce}$ :** The calculated positive- and negative-parity levels of  $^{140}\text{Ce}$  are given in Fig. 6. For the positive-parity levels comparison with the experiment is shown up to  $16^+$ . The calculated  $0_2^+$  state is higher in the calculation. The other levels are located lower than in the experiment. This nucleus has eight protons outside the core. In the  $2_1^+$ ,  $4_1^+$ ,  $6_1^+$ ,  $10_1^+$ ,  $13_1^+$ ,  $14_1^+$ ,  $15_1^+$  and  $16_1^+$  states six protons are in  $g_{7/2}$  and two are in  $d_{5/2}$  for the first four states and in  $h_{11/2}$  for the remained four states with 27.3, 28.6, 23.0, 46.1, 47.5, 50.4, 47.2 and 43.3% probabilities, respectively. For the  $6_1^+$ ,  $8_1^+$  and  $12_1^+$  states five protons are in  $g_{7/2}$  and three protons are in  $d_{5/2}$  with 38.1, 57.3, 82.1% probabilities, respectively. The  $17_1^+$  level has  $g_{7/2}^5 d_{5/2}^1 h_{11/2}^2$  configuration with 70.3% probability.

The calculated negative-parity levels show the same sequence as in the experiment. We have given two calculated eigenvalues for  $15^-$  level in order to compare with the



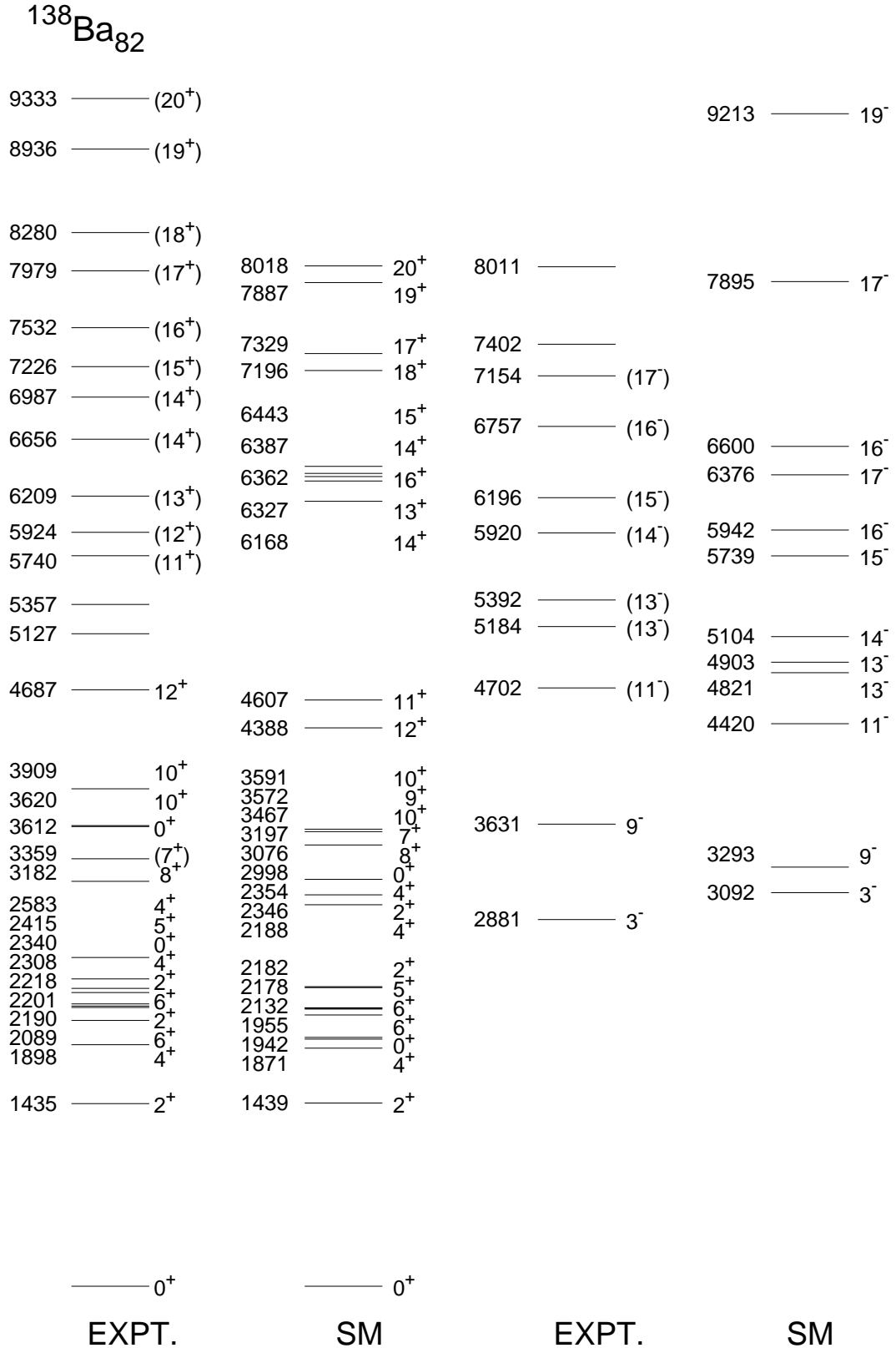


**Figure 4.** Comparison of experimental [6, 15] and calculated excitation spectra for  $^{138}\text{Ba}$  using SN100PN interaction.

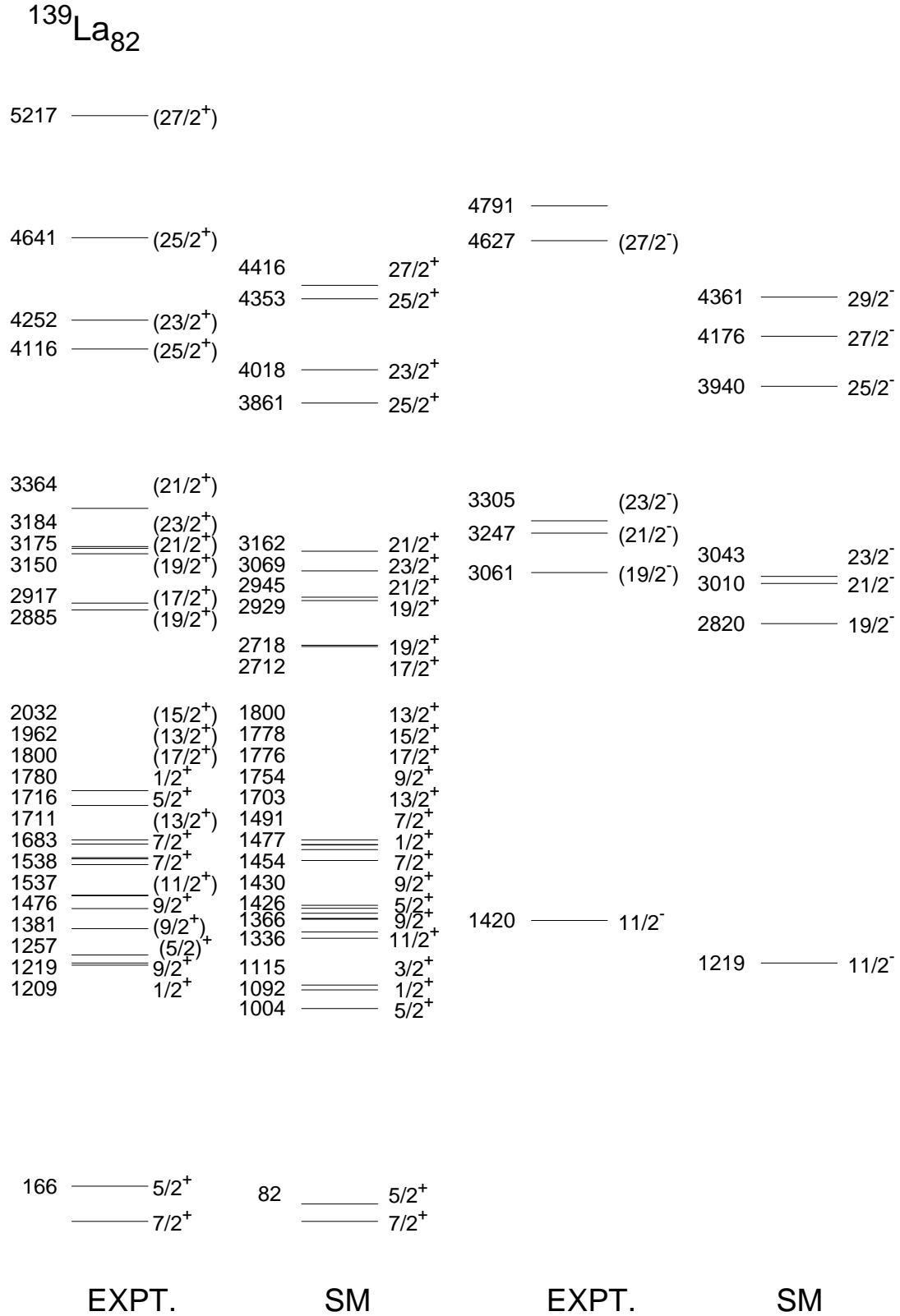


**Figure 5.** Comparison of experimental [6, 15] and calculated excitation spectra for  $^{139}\text{La}$  using SN100PN interaction.

experimental level at 5697 keV to which spin is not assigned. All the calculated levels are predicted lower than in the experiment. The negative-parity levels are produced following three configurations:  $g_{7/2}^6 d_{5/2}^1 h_{11/2}^1$  for the  $3^-$ ,  $5^-$ ,  $13^-$  and  $14^-$  states with 38.0, 24.4, 45.6 and 40.5% probabilities, respectively,  $g_{7/2}^5 d_{5/2}^2 h_{11/2}^1$  for the  $7^-$ ,  $8^-$ ,  $9^-$ ,  $11^-$ ,  $15^-$  and  $17^-$  states with, 28.4, 40.4, 40.6, 52.4, 73.2 and 79.6% probabilities, respectively and  $g_{7/2}^4 d_{5/2}^3 h_{11/2}^1$  for the  $16^-$  state with 60.3% probability.

It is important to study the configuration across  $N = 82$  gap with neutron excitations. Because from the above discussions it can be seen for  $^{136}\text{Xe}$  the experimentally observed state at 7946 keV is too low in energy to come from the  $\pi(g_{7/2}^2 d_{5/2}^2)$  configuration and for the  $^{138}\text{Ba}$  the intermediate high-spin states beyond the  $11^+$  level, the calculated results are not in a good agreement with the experiment. In  $^{137}_{55}\text{Cs}$ , the configuration of the highest-spin states is mainly from  $(\pi g_{7/2} \pi d_{5/2})^3 (\pi h_{11/2})^2$ . For this nucleus, in case of intermediate-spin, the  $(\pi g_{7/2} \pi d_{5/2})^5 (\nu h_{11/2})^{-1} (\nu f_{7/2})^{+1}$  configuration is also important. It can be noted that the difference between  $(2_1^+)$  and the ground state  $(0^+)$  energies of even isotones starting from  $^{136}\text{Xe}$  to  $^{140}\text{Ce}$  shows that it is increased by the increasing of the proton number outside  $Z = 50$  closed shell in both calculation and experiment. This is an indication of persistence of  $N = 82$  magic number for neutrons.

**Table 2.** Experimental and calculated  $B(E2)$  and  $B(E3)$  in W.u. for different transitions.

Nucleus	Transition	Expt.	Calc.
$^{136}\text{Xe}$	$B(E2; 2_1^+ \rightarrow 0_1^+)$	9.7 (4)	7.4
	$B(E2; 4_1^+ \rightarrow 2_1^+)$	1.281 (17)	0.9
	$B(E2; 6_1^+ \rightarrow 4_1^+)$	0.0132 (4)	0.089
$^{137}\text{Cs}$	$B(E2; 5/2_1^+ \rightarrow 7/2_1^+)$	>6.8	0.02
$^{138}\text{Ba}$	$B(E2; 2_1^+ \rightarrow 0_1^+)$	10.8 (5)	11.4
	$B(E2; 4_1^+ \rightarrow 2_1^+)$	0.2873(15)	0.20
	$B(E2; 6_1^+ \rightarrow 4_1^+)$	0.053(7)	0.21
	$B(E2; 2_2^+ \rightarrow 0_1^+)$	2.01(20)	0.72
	$B(E2; 4_2^+ \rightarrow 6_1^+)$	2.0(9)	1.1
$^{139}\text{La}$	$B(E2; 9/2_1^+ \rightarrow 5/2_1^+)$	1.79(24)	9.6
	$B(E2; 7/2_2^+ \rightarrow 7/2_1^+)$	11.9(16)	2.13
	$B(E2; 5/2_2^+ \rightarrow 7/2_1^+)$	19.3(22)	17.8
$^{140}\text{Ce}$	$B(E2; 2_1^+ \rightarrow 0_1^+)$	13.8(3)	14.9
	$B(E2; 0_2^+ \rightarrow 2_1^+)$	11.5(9)	6.0
	$B(E2; 4_1^+ \rightarrow 2_1^+)$	0.137(4)	0.11
	$B(E2; 6_1^+ \rightarrow 4_1^+)$	0.29(6)	0.15
	$B(E2; 10_1^+ \rightarrow 8_1^+)$	0.46(13)	0.21
	$B(E3; 3_1^- \rightarrow 0_1^+)$	27(6)	9.3

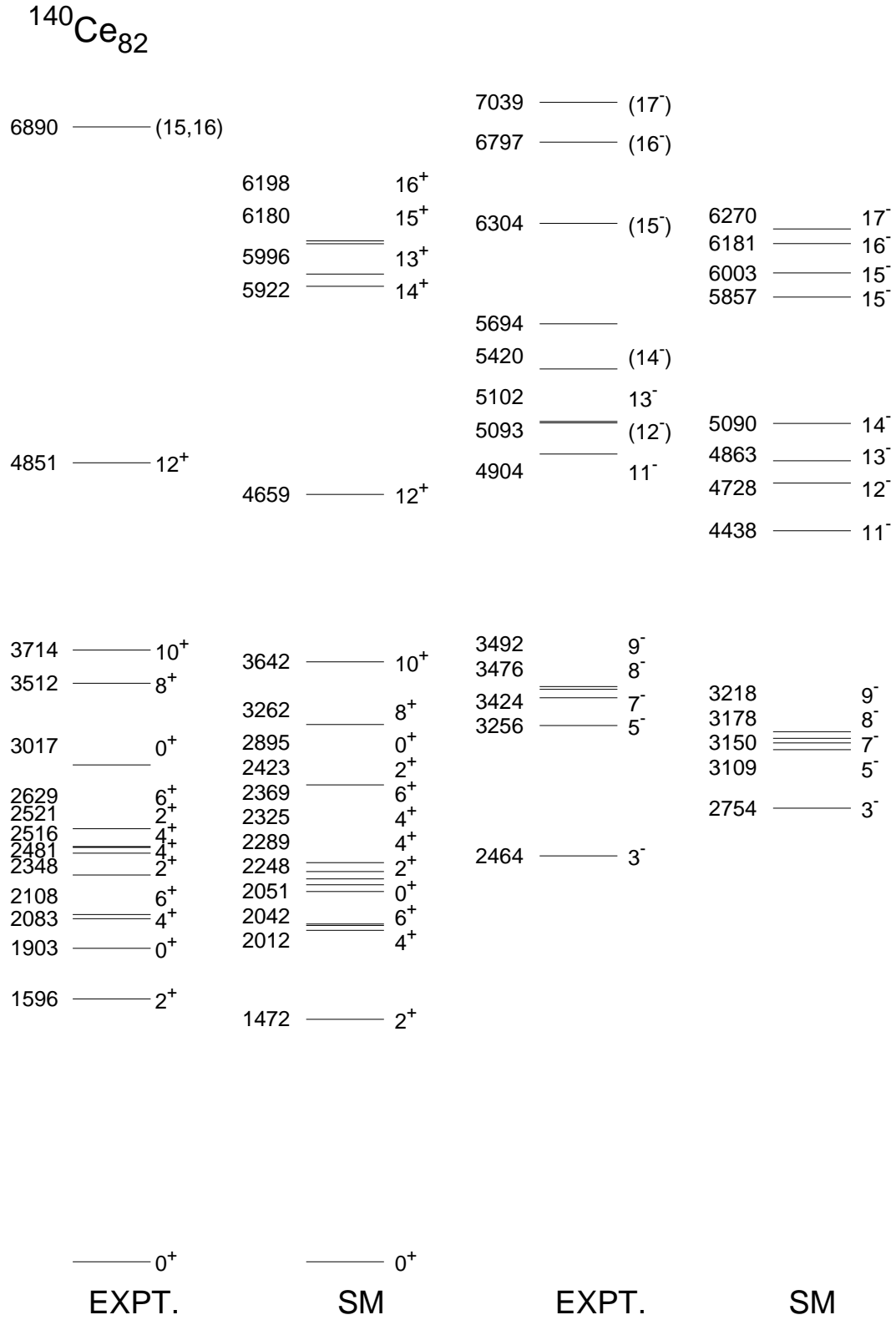


**Figure 6.** Comparison of experimental [6, 15] and calculated excitation spectra for  $^{140}\text{Ce}$  using SN100PN interaction.

### 3. Transition probability analysis

The comparison of the transition probabilities with the experiment is given in Table 2. The effective charge  $e_p=1.5$  is used in the calculation. The calculated values of  $E2$  transition probabilities are in excellent agreement with the experimental ones for the even isotones. The only  $E2$  transition existing in the experiment is measured to be more than 6.8 W.u. for the  $^{137}\text{Cs}$ . For this transition too weak  $E2$  transition is predicted by shell model. Calculations are in reasonable agreement also for the  $^{139}\text{La}$  isotone. The value of  $E2$  transition probability from  $9/2_1^+$  to  $5/2_1^+$  is predicted larger and that of from  $7/2_2^+$  to  $7/2_1^+$  is smaller as compared to the experiment. Very good agreement of the last transition is seen from the Table. We have shown in Table 2 also comparison of one calculated value of  $E3$  transition probability with its experimentally available counterpart for the  $^{140}\text{Ce}$ .

### 4. Summary

Our present work is motivated by recently available high-spin state experimental data of five  $N = 82$  isotones,  $^{136}_{54}\text{Xe}$ ,  $^{137}_{55}\text{Cs}$ ,  $^{138}_{56}\text{Ba}$ ,  $^{139}_{57}\text{La}$ , and  $^{140}_{58}\text{Ce}$  for which we performed shell model calculations. This work add more information to Refs. [2, 3] where shell model results for even  $N = 82$  isotones have been reported only up to  $J = 10^+$ . We can summarize our results by following:

- The yrast states of the five  $N = 82$  isotones are very well described by shell model.
- The results predicted by shell model for the occupancy numbers are in a very good agreement with the experimental data. The predicted numbers also show the predominance of the  $\pi g_{7/2}$ ,  $\pi d_{5/2}$  and  $\pi h_{11/2}$  orbitals. The present results for the occupancy numbers are close to the experiment in comparison to the previous shell model results.
- The structure for the positive-parity states of lighter isotones are from  $(\pi g_{7/2}\pi d_{5/2})^n$  configuration. It is found that the protons prefer to fill the  $\pi h_{11/2}$  orbital rather than  $d_{3/2}$  and  $s_{1/2}$  orbitals  $((\pi g_{7/2}\pi d_{5/2})^{n-2}(\pi h_{11/2})^2$  configuration) in the case of heavier isotones. The negative parity states are due to odd number of protons in  $\pi h_{11/2}$  orbital.
- The transition probabilities are in a good agreement with the experimental data and they are useful for understanding the structure of these isotones.
- The neutron excitations across  $N = 82$  gap is important for the intermediate-high-spin states in case of  $^{136}_{54}\text{Xe}$ ,  $^{137}_{55}\text{Cs}$ , and  $^{138}_{56}\text{Ba}$  isotones. Further theoretical development is needed by constructing a new effective interaction to enlarge the model space which at least include  $\nu f_{7/2}$  orbital from upper  $hfp_i$  shell.

*Acknowledgement:* This work was supported in part by Conacyt, México, and by DGAPA, UNAM project IN103212. MJE acknowledges support from grant No. 17901 of CONACyT projects CB2010/155633 and F2-FA-F177 of Uzbekistan Academy of

Sciences. One of the authors (P.C.S.) would like to thank to Prof. B. A. Brown for his help.

## References

- [1] Barea J, Kotila J and Iachello F 2012 *Phys. Rev. Lett.* **109** 042501
- [2] Holt A, Engeland T, Osnes E et al. 1997 *Nuclear Physics A* **618** 107
- [3] Coraggio L, Covello A, Gargano A et al. 2009 *Phys. Rev. C* **80** 044320
- [4] Zhang C T, Bhattacharyya P, Daly P J et al. 1996 *Phys. Rev. Lett.* **77** 3743
- [5] Daly P J, Bhattacharyya P, Zhang C T et al. 1999 *Phys. Rev. C* **59** 3066
- [6] Astier A, Porquet M G, Venkova T et al. 2012 *Phys. Rev. C* **85** 064316
- [7] Wimmer K, Köster U, Hoff P et al. 2011 *Phys. Rev. C* **84** 014329
- [8] Srivastava P C and Mehrotra I 2009 *Journal of Physics G: Nuclear and Particle Physics* **36** 105106
- [9] Srivastava P C and Mehrotra I 2010 *The European Physical Journal A - Hadrons and Nuclei* **45** 185
- [10] Srivastava P C 2012 *Journal of Physics G: Nuclear and Particle Physics* **39** 015102
- [11] Morales I O, Isacker P V and Talmi I 2011 *Physics Letters B* **703** 606
- [12] Wildenthal B H, Newman E and Auble R L 1971 *Phys. Rev. C* **3** 1199
- [13] Brown B A, Stone N J, Stone J R et al. 2005 *Phys. Rev. C* **71** 044317
- [14] Nushell@MSU, B. A. Brown and W. D. M. Rae, MSU-NSCL report (2007).
- [15] ENSDF database, [<http://www.nndc.bnl.gov/ensdf/>].